Doppler-shift attenuation lifetimes in ^{14}N derived from experimental stopping parameters

M. Bister, A. Anttila, and J. Keinonen
Department of Physics, University of Helsinki, Helsinki, Finland
(Received 10 February 1977)

The lifetime values of 105 ± 15, 8.4 ± 0.4 16 ± 8, and 185 ± 15 fs for the 2313, 3948, 5690, and 6204 keV levels of ^{14}N, respectively, were measured using the Doppler-shift attenuation method through the ^{13}C$(p,\gamma)^{14}$N reaction at E_p = 1150 keV. For the Doppler-shift attenuation analysis the correction factors of the nuclear and electronic stopping powers were determined by measuring Doppler-shift attenuation and line shape of γ rays from the 6204→2313 keV transition and by measuring range values of the 20, 40, 60, 80, and 100 keV ^{15}N nuclei. The two most commonly used scattering potentials, i.e., Thomas-Fermi and Lenz-Jensen, were used in the estimation of the correction factors and $F(\tau)$ curves. Both potentials were shown to give the same lifetimes. All calculations were done by the Monte Carlo method. The accuracy of the results and the transition rates in the frame of a weak coupling model are discussed.

[NUCLEAR REACTIONS ^{13}C(p,γ), E=1.15 MeV; measured E_γ, Doppler-shift attenuation. ^{14}N levels deduced, τ, Ge(Li) detector, enriched target.]

I. INTRODUCTION

Insufficient knowledge of the stopping process has been a serious problem in Doppler-shift attenuation (DSA) analysis. One way to estimate the magnitude of the error in a lifetime value has been to vary the backing material.[1,2] This procedure would yield good results if the conventionally used Lindhard-Scharff-Schiøtt (LSS) theory[3] were sufficiently reliable. Obviously, the best way would be to measure the stopping values under identical experimental conditions to those in the DSA measurements and to use these experimental data in the analysis. The nuclear physical techniques described in our earlier papers[4-6] provide suitable means for the determination of all relevant stopping parameters, in particular, for low recoil velocities. A good overall consistency for several lifetime values in ^{21}Na and ^{23}Na has been achieved[7] using these methods.

In the present work the lifetime values of four bound states in ^{14}N were remeasured using the DSA method through the ^{13}C$(p,\gamma)^{14}$N reaction. The main reason for this reanalysis was the experimental determination of the stopping power parameters, which removes the most significant error source. In addition, it was possible to improve the results by utilizing a high performance Ge(Li) detector and a new target system[8] in the measurements, while Monte Carlo calculations were used in the analysis. The effects of different scattering cross sections were studied by comparing the results of applying the Thomas-Fermi and Lenz-Jensen potentials with the lifetime derivations.

Considerable attention has been given in the literature to the low-lying states of ^{14}N. A quite recent compilation[9] gives a good description of the present situation. The improved lifetime values of the low-lying states in ^{14}N provide us with accurate isovector and isoscalar transition rates. The strong and pure electric and magnetic dipole $\Delta T = \pm 1$ transitions $2.31(J^\pi = 0^+, T = 1) \rightarrow 0(1^+, 0)$, $5.69(1^-, 0) \rightarrow 2.31(0^+, 1)$, and $6.20(1^+, 0) \rightarrow 2.31(0^+, 1)$ MeV are pure isovector transitions. The rates of the electric and magnetic dipole $\Delta T = 0$ transitions $3.95(1^+, 0) \rightarrow 0(1^+, 0)$, $5.69(1^-, 0) \rightarrow 0(1^+, 0)$, and $6.20(1^+, 0) \rightarrow 0(1^+, 0)$ MeV in the self-conjugate nucleus ^{14}N allow one to draw conclusions about isoscalar transition strengths ($M1$ transitions) and about isospin impurities ($E1$ transition).

The experimental procedure is described in Sec. II, and Sec. III presents the measurements and results. The accuracy of the results and the transition rates are discussed in Sec. IV.

II. EXPERIMENTAL PROCEDURE

A. General experimental procedure

The measurements were performed at the Helsinki University 2.5 MV Van de Graaff accelerator. Gamma rays were detected using a Princeton 110 cm^3 Ge(Li) detector (full width at half maximum = 3.2 keV at E_γ = 2.6 MeV) and analyzed with a Nuclear Data 4096 channel pulse height analyzer. The DSA measurements were performed both at the angles 0° and 90° and with the two-target system[7] at the angles 25° and 155° relative to the beam. The distances from the targets to the detector were 7 cm in the first setup and 10 cm in the second.

B. Target preparation

The targets used in the DSA measurements were prepared by implanting 40 keV $^{13}C^+$ ions into Ta in the isotope separator of the laboratory to give a ^{13}C concentration in Ta of about 20 at. %. There are several reasons for preferring the use of implanted targets, as discussed in the following. Firstly, since the abundance of ^{13}C is only 1.11%, enriched targets must be used. If the target preparation is carried out with an isotope separator, ions are normally collected onto or into some backing material with a high mass number, the heavy backing being necessary in order to avoid any disturbing reactions from the backing. If the target material is separated onto the backing, the collected layer should be thick enough to stop the recoiling ions completely in DSA measurements. However, it has been proved that the stopping cross section is dependent upon the allotropic form of carbon.[10] In addition, the stopping power of carbon is considerably lower than that of tantalum, which is a disadvantage in DSA measurements of short lifetimes. If a thin layer of carbon on a stopping backing is used, it is difficult to determine accurately the thickness of the carbon layer, and even this inaccuracy causes considerable error. A further confusing factor is the strong reflection of light ions from the heavy backing material. An alternative would be to prepare a target by evaporating enriched carbon or carbon compound onto some backing, but even then the same difficulties would arise as presented above, and in every case the stopping parameters and the density of the target would have to be determined.

If the target is prepared by implanting $^{13}C^+$ ions into Ta the only uncertain factor is their effect on on the backing. However, in the light ion implantation into Ta no significant effect has been observed.[11] This is due to the fact that as a rule, the light ions occupy interstitial positions in heavy material without expanding it significantly. In the present case, by supposing that no expansion occurs the calculated effect of <1% is consistent with the earlier experimental results.[11]

III. MEASUREMENTS AND RESULTS

A. Determination of ranges

The experimental range profiles were obtained from the broadening of the (p,γ) resonance yield curve[4,6] at the $E_p = 429$ keV resonance ($\Gamma < 1$ keV) of the $^{15}N(p,\alpha\gamma)^{12}C$ reaction.[9] The reason behind selecting ^{15}N instead of ^{14}N is the absence of any suitable resonance in ^{14}N. The $^{15}N^+$ ion implantations in Ta were made at incident energies of 20, 40, 60, 80, and 100 keV with the isotope separator of our laboratory. The doses were $(0.9\text{–}6) \times 10^{15}$ ions cm^{-2} and the dose rate was kept about 2×10^{12} ions $cm^{-2}\,s^{-1}$. Thus the concentration of ^{15}N atoms in Ta is low; at the depth corresponding to the maximum in the range distribution the concentration of ^{15}N atoms is less than 1 at. %. Two series of targets were prepared and the $(p,\alpha\gamma)$ yield measurements were made twice for each target, one set being illustrated in Fig. 1.

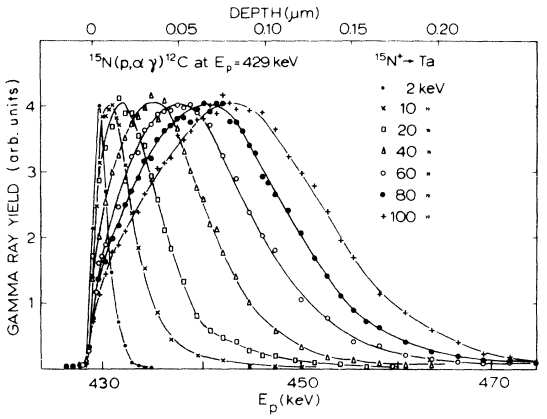

FIG. 1. The γ-ray yield curves from ^{15}N implantation into Ta backings. The peak heights are normalized to the same value, whereas the numbers of counts at the maxima varied between 2000–3000. The 2 and 10 keV curves are provided for comparison only.

The experimental range values deduced from the $^{15}N(p,\alpha\gamma)^{12}C$ yield measurements are given in Table I. In order to compare the results measured for a semi-infinite medium with the LSS theory derived for an infinite medium, Monte Carlo calculations were carried out. The range values obtained in this way are presented in the third column of Table I. The ion reflection (the factors are given in Table I) was taken into account in the Monte Carlo calculations. The estimated error for $\bar{R}_{obs}$ is ± 5%, which is mainly due to uncertainties in the proton stopping power values which had to be used in the calculations.

TABLE I. Ranges and reflection coefficients of ^{15}N in Ta.

Energy (keV)	$\bar{R}_{obs}$ ($\mu g/cm^2$)	$\bar{R}_{MC}$ [a] ($\mu g/cm^2$)	r [b] (%)
20	52	41	29
40	81	71	24
60	115	100	20
80	139	129	18
100	161	155	16

[a] Obtained with the Monte Carlo calculations and using the LSS cross sections for the stopping power.

[b] Total reflection coefficient.

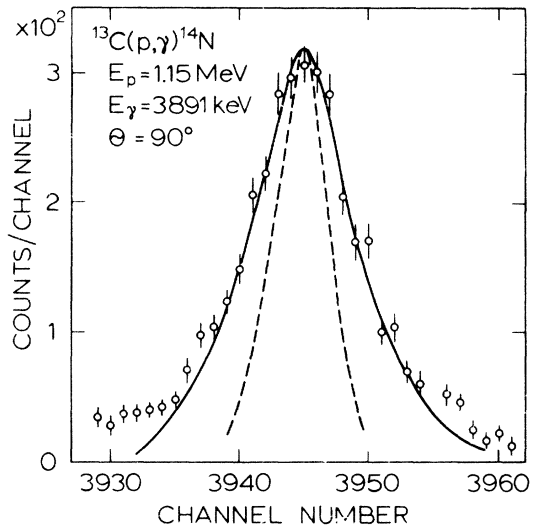

FIG. 2. The peak of the 3891 keV γ-ray measured on the tantalum backing. The solid curve is the best fit with $f_n = 0.85$ and $f_e = 1.0$. The dashed curve corresponds to the case where the emitting nuclei have the maximum velocity.

From the range results it can be observed that the $\bar{R}_{obs}$ in the energy region studied depends almost linearly on the implantation energy. Then it is evident that the energy dependences of the correction needed for the stopping power $d\epsilon/d\rho$ in the frame of the LSS theory[3] is insignificant.

B. Determination of stopping parameters

By combining the range values, the attenuation factor $F(\tau)$ obtained as the ratio of the measured Doppler shift to the calculated shift and line shape of a γ-ray peak, the correction factors f_n and f_e for the nuclear and electronic stopping, respectively, can be evaluated.[5] The stopping power is now given by $(d\epsilon/d\rho)_{corr} = f_n(d\epsilon/d\rho)_n^{LSS} + f_e(d\epsilon/d\rho)_e^{LSS}$. The F value and the shape of the 3891 keV γ-ray peak from the 6204 → 2313 keV transition were used in the present work. Figure 2 shows the best fit, which was obtained with the values $f_n = 0.85 \pm 0.05$ and $f_e = 1.0 \pm {}^{0.4}_{0.3}$. This result agrees with our earlier results for the ^{23}Na → Ta[7] and ^{27}Al → Ta[5] cases, for which $f_n = 0.75 \pm 0.05$, $f_e = 1.15 \pm {}^{0.6}_{0.3}$ and $f_n = 0.67 \pm 0.08$, $f_e = 1.0 \pm {}^{0.8}_{0.2}$, respectively, were obtained. In each case the correction factors were derived using the Thomas-Fermi potential for the scattering cross section. On the basis of these few results it would seem that the stopping parameters do not depend strongly on the implanted ions. The effects of using other scattering potentials are discussed in Sec. IV.

C. Lifetimes in ^{14}N

The $F(\tau)$ values are listed in Table II and the attenuation measurements are illustrated in Fig. 3. The corrections for solid angle attenuation were taken into account with the aid of the primary γ rays. The value $F(\tau) = 100.0 \pm 0.2\%$ was obtained for the full shift. Due to isotropic angular distribution of γ rays from the $E_p = 1150$ keV, $J^\pi = 0^+$ resonance there are no angular distribution effects on F. In the analysis of the Doppler-shift measurements, the Monte Carlo calculations and the experimental values for the stopping power parameters given above were used. The Monte Carlo calculations remove the uncertainty which otherwise arises from Blaugrund's $\langle v \rangle \langle \cos\phi \rangle$ approximation.[12] The stopping conditions during the DSA measurements are illustrated in Fig. 4. In the deduction of the calculated curve the Monte Carlo calculations were employed with the experimental knowledge of the stopping.

Direct population from the resonance level was assumed. The exception was the $E_x = 2313$ keV state whose lifetime was determined by using the

TABLE II. The mean lifetimes observed at $E_p = 1150$ keV for bound states in ^{14}N compared with previous values.

E_x (keV)	E_γ (keV)	$F(\tau)$ (%)	τ_m (fs) Present[a]	τ_m (fs) Previous[b]	τ_m (fs) Weighted average
2313	2313	21.9 ± 1.0	105 ± 15	83 ± 30	
				83 ± 19	
				114 ± 30	
				106 ± 10	102 ± 8
3948	1635	89.4 ± 0.5	8.4 ± 0.4	4.5 ± 0.4	6.5 ± 2.4
5690	3377	82 ± 8	16 ± 8	10.0 ± 2.0	10.4 ± 1.9
6204	3891	26.4 ± 0.9	185 ± 15	200 ± 45	187 ± 14

[a] Error limits also include the uncertainties due to the analysis technique.

[b] The values are as given in Ref. 9 but exclude earlier values from (p,γ) measurements.

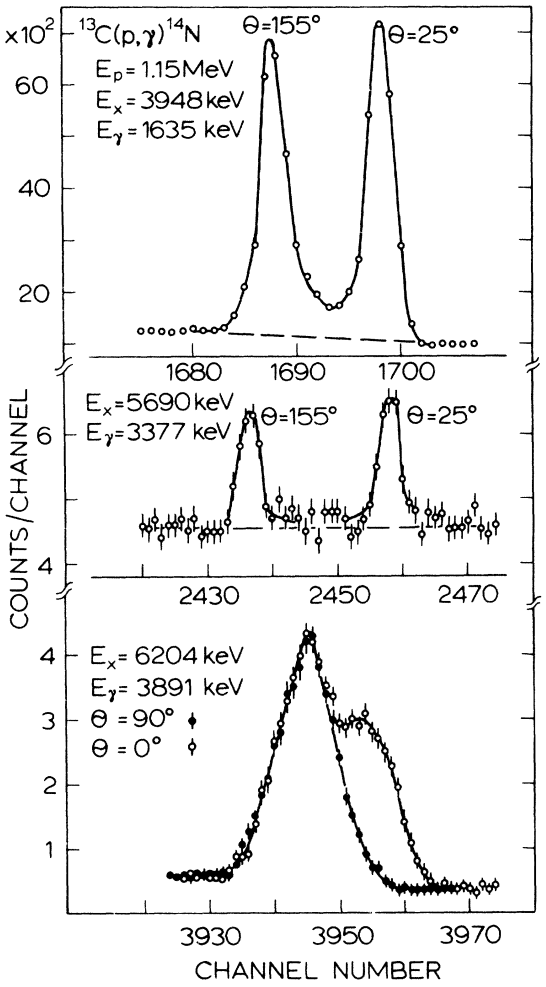

FIG. 3. Doppler-shift attenuation measurements of the three γ rays in the $^{13}C(p,\gamma)^{14}N$ reaction. The two highest cases have been measured with the two-target arrangement and the lowest one with the rotating detector system.

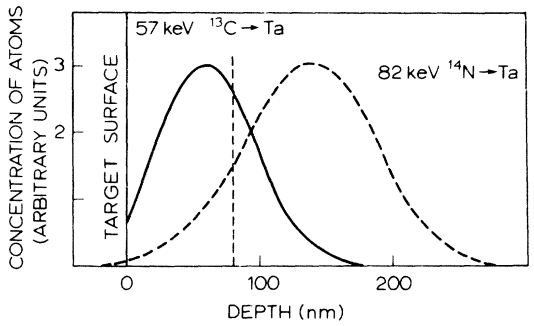

FIG. 4. Schematic diagram of the stopping conditions used in the present DSA measurement of the $E_p = 1150$ keV resonance in the $^{13}C(p,\gamma)^{14}N$ reaction. The solid curve is the experimental range profile. The vertical dashed line indicates the point at which the DSA measurement was performed. The dashed curve illustrates the range profile of the recoiling nuclei.

equation of Ref. 2 derived for the cascade cases and using the branchings given in Ref. 9. The F value for the $E_x = 3948$ keV state was measured using the conventional method whereby spectra were taken separately at angles 0° and 90° to the beam, and using the two-target system. The nearly equal $F(\tau)$ values of 89.0 ± 1.0 and $90.2 \pm 0.3\%$ were obtained, respectively. The derived lifetime $\tau = 8.4 \pm 0.4$ fs does not agree with the previous value of 4.5 ± 0.5 fs obtained from resonance scattering measurements.[9] One explanation could be the existence of a feeding γ ray from an upper state with a longer lifetime. However, according to the tabulation in Ref. 9, such transitions are not expected, as possible branchings are less than 1%. Although two 15 h runs with the two-target system were made in order to determine the F value of the $E_x = 5690$ keV state, the statistics for this state remained rather poor, Fig. 3. The result $\tau = 185 \pm 15$ fs for the $E_x = 6204$ keV state is in good agreement with the value of 200 ± 45 fs obtained in the high recoil velocity DSA measurements.[13] On the other hand, the present value disagrees with our previous value of 118 ± 7 fs[2] which was an average of the results obtained with several backing materials. However, the value of 155 ± 30 fs[2] obtained earlier using a Ta backing agrees well with the present one, because the difference between the LSS theory and experiment happens to be small in this case. The result $\tau = 105 \pm 15$ fs for the $E_x = 2313$ keV state is a little longer than the tabulation value of 85 ± 5 fs,[9] but is in excellent agreement with the recent bremsstrahlung scattering result 106 ± 10 fs reported by Rasmussen and Metzger.[14]

IV. DISCUSSION

A. Accuracy of the results

The use of constant correction factors f_n and f_e in the stopping power, ignoring their possible energy and scattering angle dependence should, of course, be considered as a first order correction. Thus our method of determining f_n and f_e, where the energy varies between different limits in different measurements, may reduce the accuracy of our f_n and f_e. However, it seems that this is not so serious in practice, because the calculated ranges for different energies using our constant f_n and f_e agree well with the experimental values.

It is obvious that different screening potentials yield different f_n and f_e values and more important, possibly also different lifetimes. In order to check the significance of this effect an additional calculation of f_n, f_e, and τ was done using the Lenz-

Jensen potential in the $\tau = 185$ fs case. Whereas f_n changed from 0.85 to 0.95, the change in τ and f_e was insignificant. Also in this case the calculated ranges are consistent with experiment within the error limits.

If the lifetime is short, the line shape of the γ ray at 90° is not broadened enough for determination of f_n, f_e, and τ. Fortunately, in the cases considered so far, the range and DSA measurements fix f_n, f_e, and τ so that different possible f_n and f_e combinations have almost the same τ. In principle it might be expected that anomalies in the f_n values as a function of energy and scattering angle could occur. However, no anomalies were found in the observed range values and, because there is no clear reason for strong variations in the f_e values, no significant change in the f_n value is expected.

Further, the good consistency of our present and earlier results with those obtained from different methods would indicate that there are no other serious sources of error. The only exception is the result of 8.5 ± 0.4 fs for the 3948 keV state, which clearly disagrees with the value 4.5 ± 0.4 fs obtained from electron scattering.

B. Transition strengths

The low-lying state of ^{14}N have been described mainly by the $1s^4 1p^{10}$ configuration.[9] Due to the vicinity of ^{16}O the spectrum of ^{14}N has been calculated with a weak coupling model.[15] In the calculations based upon weak coupling of particles in the *sd* shell and holes in the *p* shell a good fit to the experimental data has been obtained. The present experimental transition strengths are given in Table III along with the predictions of the weak coupling model.

The transition matrix element of an electromagnetic transition with the nuclear system going from state i to state f in the self-conjugate nucleus ^{14}N is, in the isospin formalism,[16] given by

$$\langle f|H|i\rangle = \begin{pmatrix} T_f & 0 & T_i \\ -T_f & 0 & T_i \end{pmatrix} \langle J_f M_f; T_f \,||H_0||\, J_i M_i; T_i\rangle + \begin{pmatrix} T_f & 1 & T_i \\ -T_f & 0 & T_i \end{pmatrix} \langle J_f M_f; T_f \,||H_1||\, J_i M_i; T_i\rangle .$$

It can be seen from the 3-j symbols that for $\Delta T = \pm 1$ transitions only the isovector part contributes. The weak coupling model reproduces well the pure $M1$ transition $2.31(J^\pi = 0^+, T = 1) \rightarrow 0(1^+, 0)$ MeV. The prediction of the main branch $3.95(1^+, 0) \rightarrow 2.31(0^+, 1)$, which is also a pure $M1$ transition, is too high by a factor of 1.6. In the case of the third pure $M1$ transition $6.20(1^+, 0) \rightarrow 2.31(0^+, 1)$ MeV the weak coupling model overestimates the strength by a factor of 60. The initial $J^\pi = 1^+$, $T = 0$ levels have been assumed to be predominantly 0p-2h states to which a 2p-4h configuration has been added. The disagreement between the present experimental value and the weak coupling model predictions suggests alterations to the configurations used. In particular, the experimental strength value of the $6.20(1^+, 0) \rightarrow 2.31(0^+, 1)$ MeV transition, not known in Ref. 15, confirms the introduction of a tensor force for the particle-hole interaction as discussed by Lie.[15] The prominent and pure $E1$ decay $5.69(1^-, 0) \rightarrow 2.31(0^+, 1)$ MeV is overestimated by a factor of 13 in this model. The $5.69(1^-, 0)$ MeV state is described as an almost pure 1p-3h state, as for all states below 12 MeV. Because the 3p-5h configurations which lie at very high energies have only very small influence on this state, the reduction can be explained by additive admixture in the configuration of the $2.31(0^+, 1)$ MeV state. This could also be an explanation for the disagreements

TABLE III. Experimental transition strengths of bound states in ^{14}N and their comparison with a weak coupling model 15. Mean lives are weighted averages from Table II, other assignments are taken from Ref. 9.

E_i (MeV)	E_f (MeV)	J_i^π, T_i	J_f^π, T_f	τ_m (fs)	Branching (%)	Multipolarity	Γ_γ/Γ_w (W.u.) Exp.	Γ_γ/Γ_w (W.u.) Weak coupling model
2.31	0	$0^+, 1$	$1^+, 0$	102 ± 8	100	$M1$	$(2.5 \pm 0.2) \times 10^{-2}$	2.7×10^{-2}
3.95	0	$1^+, 0$	$1^+, 0$	6.5 ± 2.4	3.9 ± 0.2	$M1$	$(3.5 \pm 1.4) \times 10^{-4}$ [a]	3.1×10^{-4}
						$E2$	(2.3 ± 0.8)	2.6(0)
	2.31		$0^+, 1$		96.1 ± 0.3	$M1$	(1.1 ± 0.4)	1.74(0)
5.69	0	$1^-, 0$	$1^+, 0$	10.4 ± 1.9	35.6 ± 1.2	$E1$	$(3.1 \pm 0.6) \times 10^{-4}$	9.7×10^{-4}
	2.31		$0^+, 1$		63.1 ± 1.2	$E1$	$(2.6 \pm 0.5) \times 10^{-3}$	3.5×10^{-2}
6.20	0	$1^+, 0$	$1^+, 0$	187 ± 14	23.0 ± 1.9	$M1$	$(1.6 \pm 0.2) \times 10^{-4}$ [b]	5.3×10^{-5}
						$E2$	$(1.9 \pm 0.8) \times 10^{-3}$	3.7×10^{-1}
	2.31		$0^+, 1$		76.7 ± 2.0	$M1$	$(2.2 \pm 0.2) \times 10^{-3}$	1.3×10^{-1}

[a] $\delta = -2.80 \pm 0.27$.
[b] $\delta = +0.19 \pm 0.04$.

mentioned above. Since the $M1$ ground state transition $2.31(0^+,1) \rightarrow 0(1^+,0)$ MeV, which is in agreement with the experimental value, can be explained well within the 0p-2h configuration,[17] we suggest that the information about the required 2p-4h admixture can be extracted from the $3.95 \rightarrow 2.31$, $6.20 \rightarrow 2.31$, and $5.69 \rightarrow 2.31$ MeV transitions.

From the 3-j symbols one can also see that for $\Delta T = 0$ transition the isovector contribution vanishes so that the transition strength depends only on the isovector part. Further, due to the isoscalar part of the $E1$ operator, the matrix element of this transition is zero.[16] As the possible $M2$ admixture does not introduce any significant correction to the transition rate, the strength obtained for the $5.69(1^-,0) \rightarrow 0(1^+,0)$ MeV transition indicates the isospin mixture of other negative parity states, as explained in Ref. 15. The present strength differs by a factor of 3 from the weak coupling estimate and suggests alterations to the configurations used. The isoscalar part of the $M1$ transition is expected to be weaker than the average $M1$ transition strength[18] 0.49 Weisskopf units (W.u.) by a factor of 100[16]. The $M1$ strengths obtained are in agreement with this rough rule. The strength of the $3.95(1^+,0) \rightarrow 0(1^+,0)$ MeV transition is well predicted in the weak coupling model. The large discrepancy in the strengths of the $6.20(1^+,0) \rightarrow 0(1^+,0)$ MeV transition suggests further alterations to the configurations of these levels.

[1] C. Broude, P. Engelstein, M. Popp, and P. N. Tandon, Phys. Lett. 39B, 185 (1972).
[2] M. Bister, A. Anttila, M. Piiparinen, and M. Viitasalo, Phys. Rev. C 3, 1972 (1971).
[3] J. Lindhard, M. Scharff, and H. E. Schiøtt, K. Dan. Vidensk. Selsk., Mat.-Fys. Medd. 33, No. 14, (1963).
[4] M. Bister, A. Anttila, A. Fontell, and E. Leminen, Z. Phys. 250, 82 (1972).
[5] M. Bister, A. Anttila, and J. Keinonen, Phys. Lett. 53A, 471 (1975).
[6] A. Anttila, M. Bister, A. Fontell, and B. Winterbon, Radiat. Eff. (to be published).
[7] A. Anttila, M. Bister, and J. Keinonen, Z. Phys. A274, 227 (1975).
[8] A. Anttila, J. Keinonen, and M. Bister, Nucl. Instrum. Methods 124, 605 (1975).
[9] F. Ajzenberg-Selove, Nucl. Phys. A268, 1 (1976).
[10] S. Matteson, E. K. L. Chau, and D. Powers, Phys. Rev. A 14, 169 (1976).
[11] M. Bister and A. Anttila, Nucl. Instrum. Methods 77, 315 (1970).
[12] A. E. Blaugrund, Nucl. Phys. 88, 501 (1966).
[13] F. Haas, R. M. Freeman, B. Heusch, S. Kohmoto, and A. Gallman, Nucl. Phys. A211, 289 (1973).
[14] W. K. Rasmussen and F. R. Metzger, Phys. Rev. C 12, 706 (1975).
[15] S. Lie, Nucl. Phys. A181, 517 (1972).
[16] E. K. Warburton and J. Weneser, in *Isospin in Nuclear Physics*, edited by D. H. Wilkinson (North-Holland, Amsterdam, 1969), p. 173.
[17] H. J. Rose, O. Häusser, and E. K. Warburton, Rev. Mod. Phys. 40, 591 (1968).
[18] S. K. Skorka, J. Hertel, and T. W. Retz-Schmidt, Nucl. Data A2, 347 (1966).